Polymer Chemistry

RSC Publishing

COMMUNICATION

View Article Online
View Journal | View Issue

Cross-linkable aggregation induced emission dye based red fluorescent organic nanoparticles and their cell imaging applications†

Cite this: *Polym. Chem.*, 2013, **4**, 5060

Received 2nd July 2013
Accepted 25th July 2013

DOI: 10.1039/c3py00860f

www.rsc.org/polymers

Xiqi Zhang,‡*[a] Meiying Liu,‡[b] Bin Yang,[a] Xiaoyong Zhang,[a] Zhenguo Chi,[c] Siwei Liu,[c] Jiarui Xu[c] and Yen Wei*[a]

A cross-linkable aggregation induced emission (AIE) dye (named as R-E) with two vinyl end groups was facilely incorporated into polymer nanoparticles through reversible addition–fragmentation chain transfer polymerization. Thus obtained polymeric nanoparticles showed uniform size, high water dispersibility, strong red fluorescence and excellent biocompatibility, making them promising for cell imaging applications.

Since the first reported aggregation induced emission (AIE) phenomenon by Tang *et al.* in 2001,[1] a variety of AIE dyes including tetraphenylethene,[2–6] siloles,[7,8] cyano-substituted diarylethene,[9] triphenylethene,[10–14] and distyrylanthracene[15–17] derivatives have been synthesized and extensively investigated for potential applications in fields ranging from bio/chem sensors, optoelectronic devices and bioimaging.[18–27] In particular, the fabrication of AIE dye based bioprobes and their biomedical applications have recently attracted increasing interest because of their attractive AIE characteristics, biodegradability and biocompatibility.[28–36] Many strategies for fabrication of AIE based fluorescent organic nanoparticles (FONs) have been developed. For example, Tang and Liu have demonstrated that hydrophobic AIE dyes could be facilely incorporated into a biocompatible biomolecule (bovine serum albumin), and thus obtained AIE based FONs showed high water stability and good biocompatibility, and have been successfully utilized for bioimaging applications *in vitro* and *in vivo*.[37] Furthermore, the encapsulation of AIE dye (**An18**) into commercial surfactants (F127), synthetic copolymers and inorganic nanoparticles has also been reported and extensively explored for biomedical applications.[38–43] Despite many impressive advances, the design and synthesis of novel AIE based FONs, which possess high water dispersibility, good controllability, remarkable optical properties, excellent biocompatibility and biodegradability, are still highly desirable.

Polymerization is an important method which has been previously used for fabrication of FONs *via* controllable incorporation of polymerizable organic dyes into polymers. A series of FONs based on polymerizable organic dyes have been reported and showed high potential in a variety of fields.[44] The general force for formation of these FONs can be ascribed to the self-assembly of these amphiphilic copolymers in aqueous solution. During the self-assembly procedure, hydrophobic segments including organic dyes are encapsulated in the core, while the hydrophilic segments are covered on the hydrophobic core as the shell, which can be extended into water with high water dispersibility. However, the fluorescent intensity of thus obtained FONs will be significantly weakened in aqueous solution because of the notorious aggregation-caused quenching (ACQ) effect.[35] On the other hand, FONs prepared *via* self-assembly are often unstable in physiological solution due to the weak interactions among these amphiphilic fluorescent molecules.[36] To this end, the incorporation of cross-linkable AIE dyes into copolymers *via* controlled polymerization is expected to simultaneously overcome both the problems described above. Polyethylene glycol (PEG) is a commercial available amphiphilic polymer which has been approved by the U.S. Food and Drug Administration (FDA) to supplement for many biomedical applications a long time ago. Because of its high water solubility, non-immunogenicity, bioinertness and biocompatibility,

[a]*Department of Chemistry and the Tsinghua Center for Frontier Polymer Research, Tsinghua University, Beijing, 100084, P. R. China. E-mail: sychyzhang@126.com; weiyen@tsinghua.edu.cn*

[b]*Beijing National Laboratory for Molecular Sciences (BNLMS), Key Laboratory of Organic Solids, Laboratory of New Materials, Institute of Chemistry, Chinese Academy of Sciences, Beijing 100190, China*

[c]*PCFM Lab, DSAPM Lab and KLGHEI of Environment and Energy Chemistry, FCM Institute, State Key Laboratory of Optoelectronic Materials and Technologies, School of Chemistry and Chemical Engineering, Sun Yat-sen University, Guangzhou 510275, China*

† Electronic supplementary information (ESI) available: Detailed information about the synthetic route, ^{1}H NMR, IR and HRMS of **R-E**; preparation of **R-PEG** FONs; the AIE characteristics of **R-E**; photographs of **R-PEG** FONs in water dispersion; PL spectra of **R-PEG** in different solvents; PL spectra and biocompatibility evaluations of **R-PEG-40** FONs; CLSM images of A549 cells incubated with **R-PEG-40** FONs. See DOI: 10.1039/c3py00860f

‡ These authors contributed equally to this work.

PEG has been widely utilized for surface modification of inorganic and organic nanoparticles to render them better performance. It has been demonstrated that PEGylated nanoparticles are expected to exhibit improved water dispersibility, enhancement of biocompatibility and long circulation time.[45,46]

In this work, a novel strategy for fabrication of AIE based FONs was developed for the first time, based on the cross-linkable AIE dye (named as **R-E**) and a water soluble monomer poly(ethylene glycol) monomethyl ether methacrylate (PEGMA, M_n = 950 Da) using reversible addition–fragmentation chain transfer polymerization (RAFT). Thus obtained FONs were cross-linked by **R-E** due to its two inherent polymerizable C=C bonds. Finally, the biocompatibility and cell uptake behavior of thus obtained FONs were further determined to evaluate their potential for cell imaging applications (Scheme 1).

The AIE fluorogen **R-E** was prepared following the synthetic route as described in the ESI (Scheme S1†). Its structure was characterized and confirmed by standard spectroscopic methods (in ESI†), which suggested that **R-E** was successfully synthesized. The AIE characteristics of **R-E** are shown in Fig. S1.† To prepare **R-PEG** FONs, the hydrophobic AIE dye (**R-E**) was copolymerized with an amphiphilic monomer PEGMA through RAFT polymerization (Scheme 2). Based on the feed molar ratio, the designed degrees of polymerization (DP) for copolymers are 20 and 40, and the ratio of monomer PEGMA to **R-E** is 10 : 1. Based on the designed DP, these copolymers were named as **R-PEG-20** (DP = 20) and **R-PEG-40** (DP = 40). The number average molecular weights (M_ns) of these copolymers were determined by gel permeation chromatography (GPC). Results showed that the M_ns for **R-PEG-20** and **R-PEG-40** are 29 016 and 35 673 Da respectively with a narrow polydispersity index (1.17 for **R-PEG-20** and 1.25 for **R-PEG-40**). Due to the hydrophobic feature of **R-E**, such obtained copolymers showed amphiphilic properties. When they were dispersed in aqueous solution, these copolymers tended to self-assemble into nanoparticles, the cores of which were the aggregates of **R-E** and surfaces were covered with PEGMA. Therefore, thus obtained nanoparticles are expected to exhibit strong fluorescence and high dispersibility in aqueous solution.

Fig. 1A and B show the representative transmission electron microscopy (TEM) images of **R-PEG** FONs. Many spherical nanoparticles with diameters of a few hundred nanometers can be clearly identified. The TEM images give direct evidence that copolymers self-assembled into nanoparticles in aqueous solution. Although the properties of copolymers could be well adjusted through RAFT polymerization, the size and morphology of **R-PEG** FONs are difficult to control due to the complexity of the self-assembly procedure. As compared with Fig. 1A and B, no significant differences were found between the sizes of **R-PEG-20** and **R-PEG-40**. On the other hand, the hydrodynamic size distributions of **R-PEG-20** and **R-PEG-40** in water and phosphate buffer solution (PBS) were also determined. Results showed that the size distributions of **R-PEG-20** and **R-PEG-40** in pure water were 283.8 ± 12.4 nm and 117.2 ± 5.7 nm, respectively, while their size distributions in PBS increased to 293.4 ± 2.6 and 152.4 ± 3.9 nm for **R-PEG-20** and **R-PEG-40**, respectively. The disparity of size distributions of **R-PEG-20** and **R-PEG-40** may be due to the different molecular aggregation states caused by the various crosslinking degrees of the polymer. The stability of the FONs was characterized by zeta potential measurements using ZetaPlus apparatus (Brookhaven Instruments, Holtsville, NY). The results showed zeta-potentials

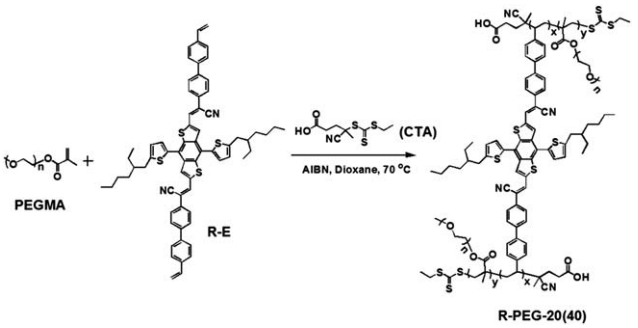

Scheme 2 Synthetic routes to **R-PEG-20** and **R-PEG-40** *via* reversible addition–fragmentation chain transfer (RAFT) polymerization using **R-E** and PEGMA as the monomers.

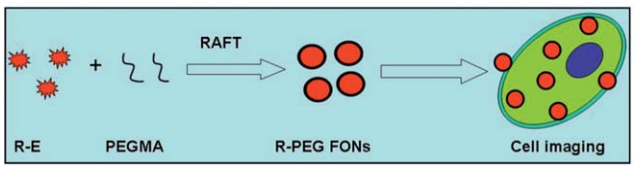

Scheme 1 Schematic showing the preparation of **R-PEG** FONs through reversible addition–fragmentation chain transfer (RAFT) polymerization and cell imaging applications of thus obtained **R-PEG** FONs.

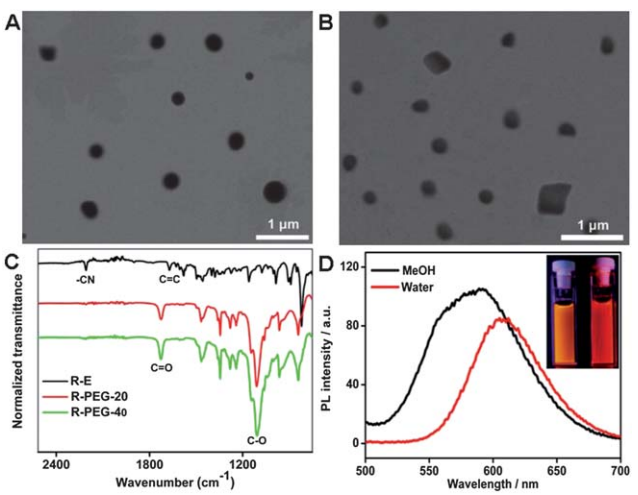

Fig. 1 Characterization of **R-E** and **R-PEG** FONs. (A and B) TEM images of **R-PEG-20** (A) and **R-PEG-40** (B) FONs; images show that the diameters of **R-PEG** FONs are about a few hundred nanometers, (C) normalized IR spectra of **R-E** and **R-PEG** FONs, a strong stretching vibration band of C=O which is located at 1732 cm^{-1} and a C–O stretching vibration band which is located at 1108 cm^{-1} were observed for the sample of **R-PEG** FONs, suggesting that **R-PEG** FONs were formed. (D) PL spectra of **R-PEG** FONs (in methanol and water), the excitation wavelength is 365 nm. Insets show fluorescent images of **R-PEG** FONs (left bottle (in methanol), right bottle (in water)) under a UV lamp (λ = 365 nm).

of -29.2 ± 1.6 mV and -31.3 ± 1.1 mV for **R-PEG-20** and **R-PEG-40** in PBS respectively, which demonstrated the stability of the **R-PEG** FONs. The successful synthesis of **R-PEG** copolymers was also confirmed by Fourier transform infrared spectroscopy (FT-IR). As shown in Fig. 1C, a characteristic peak located at 1672 cm^{-1} was observed in the sample of **R-E**, evidencing that the stretching vibration band of C=C existed in **R-E**. Furthermore, a series of peaks distributed between 1450 and 1600 cm^{-1} ascribed to the stretching vibration of polycyclic aromatic rings was also identified in the sample of **R-E**. After polymerization, a strong stretching vibration band of C=O located at 1732 cm^{-1} was observed in **R-PEG** FONs. On the other hand, a characteristic peak centered at 1108 cm^{-1} was also observed in copolymers, evidencing that C–O was introduced into the copolymers. More importantly, the stretching vibration band of C=C located at 1672 cm^{-1} disappeared after polymerization, further confirming the successful formation of copolymers. Due to the amphiphilic properties of **R-PEG** copolymers, they tended to self-assemble into nanoparticles. The hydrophobic AIE dyes (**R-E**) were expected to be encapsulated in the core of nanoparticles while the hydrophilic monomers (PEGMA) covered the hydrophobic core thus giving them high water dispersibility (Fig. S2†). Due to the aggregation of **R-E** in their core, **R-PEG** FONs showed strong fluorescence in pure water (right bottle of insets in Fig. 1D). The PL spectra of **R-PEG-20** in methanol and pure water are shown in Fig. 1D. As compared with the FONs in methanol, the wavelength of **R-PEG-20** in water red-shifted from 591 to 612 nm (Fig. 1D and insets of Fig. 1D). This red-shifted phenomenon is mainly caused by the increased solvent polarity. To find the evidence of the relationship between red-shift and solvent polarity, the emission spectra of **R-PEG-20** were recorded in solvents with different polarities (Fig. S3†). The results demonstrated that when the polarity of the solvent was increased, the emission wavelength of the **R-PEG-20** red-shifted. Similar results were found for **R-PEG-40** (Fig. S4 and S5†). The PL intensity of **R-PEG-20** in MeOH and water showed different trends from that of **R-PEG-40**, this may be due to the different effects of solvent polarity and the molecular aggregation.

The biocompatibility was examined to evaluate the potential biomedical applications of **R-PEG** FONs.[47–53] First, the influences of **R-PEG** FONs to A549 cells were examined by optical microscopy after cells were incubated with different concentrations of **R-PEG** FONs for 24 h. As shown in Fig. 2A–C, no significant differences were found between the control cells (Fig. 2A) and cells incubated with 40 (Fig. 2B) and 80 μg mL^{-1} (Fig. 2C) of **R-PEG** FONs. These results suggested that the FONs are biocompatible with cells. To further confirm the cytocompatibility of **R-PEG** FONs, the cell viability of A549 cells incubated with **R-PEG** FONs was determined by the cell counting kit-8 (CCK-8) assay as described in our previous reports.[54–57] As shown in Fig. 2D, no cell viability decrease was observed when cells were incubated with 10–80 μg mL^{-1} of **R-PEG** FONs. The cell viability value is still greater than 90% even when the concentration is up to 80 μg mL^{-1}. And no significant difference was observed between **R-PEG-20** and **R-PEG-40**. These results suggested that these FONs have high potential for biomedical applications. More importantly, the excellent biocompatibility

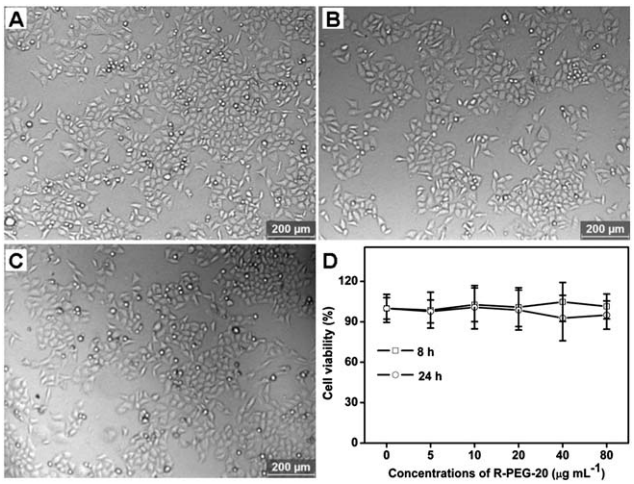

Fig. 2 Biocompatibility evaluations of **R-PEG** FONs. (A–C) Optical microscopy images of A549 cells incubated with different concentrations of **R-PEG** FONs for 24 h, (A) control cells, (B) 40 μg mL^{-1}, (C) 80 μg mL^{-1}, (D) cell viability of **R-PEG-20** with A549 cells. The biocompatibility evaluation suggested that **R-PEG** FONs were biocompatible enough for biomedical applications.

could be expected due to their surface covered with PEG, which has been previously demonstrated to be biocompatible with living organisms. In our previous reports, FONs based on AIE dye (**An18**) and commercial surfactant (F127)/synthetic copolymers have also been demonstrated.[38,39] Compared with previous reported molecules, the FONs fabricated by the method in this work have some obvious advantages. First, the AIE dye (**R-E**) was covalently incorporated into the copolymers for the formation of a cross-linkable copolymer. It should be more stable than that formed by self-assembly. On the other hand, many functional groups could be facilely incorporated into AIE based FONs *via* using different monomers. Therefore, many other components including drugs, imaging agents and targeting agents could be further integrated into the AIE based FONs. Thus multifunctional imaging and therapy platform based on **R-PEG** FONs can be facilely fabricated *via* controlled polymerization of cross-linkable AIE dyes.

Based on the biocompatibility results, cell imaging applications of **R-PEG** FONs were further explored. The cell uptake behavior of **R-PEG** FONs was evaluated by Confocal Laser Scanning Microscopic (CLSM) observation.[58–60] As shown in Fig. 3 and S7,† strong fluorescence could be observed at the cell

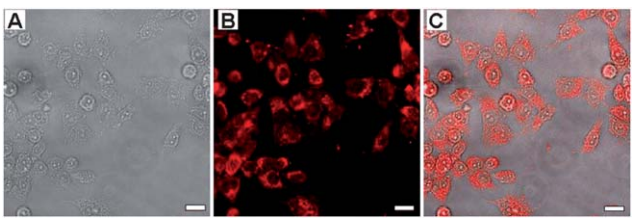

Fig. 3 CLSM images of A549 cells incubated with 10 μg mL^{-1} of **R-PEG-20** FONs for 3 h. (A) Bright field, (B) excited with a 543 nm laser, (C) merge image of (A) and (B). Scale bar = 20 μm.

location after they were incubated with 40 μg mL^{-1} of **R-PEG** FONs. Furthermore, the areas with relatively weak fluorescence intensity are possibly the location of the cell nuclei (Fig. 3B). These results suggested facile uptake of **R-PEG** FONs by cells which are mainly located at the cytoplasm. As compared with the size of FONs and nucleus pore, we believe that these FONs could not enter the cell nucleus directly. More importantly, due to the intense fluorescence of **R-PEG** FONs, strong signal could be detected after cells were incubated with 40 μg mL^{-1} of **R-PEG** FONs for 3 h, and the dosage can be further decreased if FONs were conjugated with targeting molecules. Based on the cell viability results, we believe that **R-PEG** FONs are biocompatible enough for bioimaging applications. Taking advantage of the merits of **R-E** and PEG, thus obtained **R-PEG** FONs described in this work should be of great potential for biomedical applications.

In summary, red **R-PEG** FONs were prepared *via* copolymerization of cross-linkable AIE dye (**R-E**) and PEGMA through RAFT polymerization. Thus obtained copolymers with amphiphilic properties tended to self-assemble into uniform FONs with diameters of about a few hundred nanometers. Due to their surfaces covered with PEGMA, **R-PEG** FONs showed high dispersibility and strong fluorescence in the aqueous environment. Biocompatibility evaluation suggested that **R-PEG** FONs were biocompatible enough for bioimaging applications. More importantly, various AIE based FONs could be easily fabricated *via* using different AIE dyes and monomers. And the FONs can be further conjugated with other components such as drugs, imaging agents and targeting agents, thus multifunctional theranostic systems can be fabricated. Considering their excellent properties, thus obtained FONs are expected to have high potential for various biomedical applications.

Acknowledgements

This research was supported by the National Science Foundation of China (no. 21134004, 21201108), and the National 973 Project (no. 2011CB935700), China Postdoctoral Science Foundation (2012M520243, 2013T60100, 2012M520388, 2013T60178).

References

1 J. Luo, Z. Xie, J. W. Y. Lam, L. Cheng, H. Chen, C. Qiu, H. S. Kwok, X. Zhan, Y. Liu, D. Zhu and B. Z. Tang, *Chem. Commun.*, 2001, 1740–1741.
2 X. Zhang, Z. Chi, H. Li, B. Xu, X. Li, W. Zhou, S. Liu, Y. Zhang and J. Xu, *Chem.–Asian J.*, 2011, **6**, 808–811.
3 X. Zhang, Z. Chi, H. Li, B. Xu, X. Li, S. Liu, Y. Zhang and J. Xu, *J. Mater. Chem.*, 2011, **21**, 1788–1796.
4 X. Zhang, Z. Chi, Y. Zhang, S. Liu and J. Xu, *J. Mater. Chem. C*, 2013, **1**, 3376–3390.
5 R. Hu, C. A. Gómez-Durán, J. W. Lam, J. L. Belmonte-Vázquez, C. Deng, S. Chen, R. Ye, E. Peña-Cabrera, Y. Zhong and K. S. Wong, *Chem. Commun.*, 2012, **48**, 10099–10101.
6 X. Li, X. Zhang, Z. Chi, X. Chao, X. Zhou, Y. Zhang, S. Liu and J. Xu, *Anal. Methods*, 2012, **4**, 3338–3343.
7 Y. Yu, C. Feng, Y. Hong, J. Liu, S. Chen, K. M. Ng, K. Q. Luo and B. Z. Tang, *Adv. Mater.*, 2011, **23**, 3298–3302.
8 Z. Li, Y. Q. Dong, J. W. Lam, J. Sun, A. Qin, M. Häußler, Y. P. Dong, H. H. Sung, I. D. Williams and H. S. Kwok, *Adv. Funct. Mater.*, 2009, **19**, 905–917.
9 B. K. An, S. K. Kwon, S. D. Jung and S. Y. Park, *J. Am. Chem. Soc.*, 2002, **124**, 14410–14415.
10 X. Zhang, Z. Yang, Z. Chi, M. Chen, B. Xu, C. Wang, S. Liu, Y. Zhang and J. Xu, *J. Mater. Chem.*, 2010, **20**, 292–298.
11 X. Zhang, Z. Chi, B. Xu, H. Li, Z. Yang, X. Li, S. Liu, Y. Zhang and J. Xu, *Dyes Pigm.*, 2011, **89**, 56–62.
12 X. Li, Z. Chi, B. Xu, H. Li, X. Zhang, W. Zhou, Y. Zhang, S. Liu and J. Xu, *J. Fluoresc.*, 2011, **21**, 1969–1977.
13 X. Zhang, Z. Chi, B. Xu, H. Li, W. Zhou, X. Li, Y. Zhang, S. Liu and J. Xu, *J. Fluoresc.*, 2011, **21**, 133–140.
14 C. Chen, J.-Y. Liao, Z. Chi, B. Xu, X. Zhang, D.-B. Kuang, Y. Zhang, S. Liu and J. Xu, *RSC Adv.*, 2012, **2**, 7788–7797.
15 X. Zhang, Z. Chi, J. Zhang, H. Li, B. Xu, X. Li, S. Liu, Y. Zhang and J. Xu, *J. Phys. Chem. B*, 2011, **115**, 7606–7611.
16 X. Zhang, Z. Chi, X. Zhou, S. Liu, Y. Zhang and J. Xu, *J. Phys. Chem. C*, 2012, **116**, 23629–23638.
17 X. Zhang, Z. Chi, B. Xu, L. Jiang, X. Zhou, Y. Zhang, S. Liu and J. Xu, *Chem. Commun.*, 2012, **48**, 10895–10897.
18 X. Feng, L. Liu, S. Wang and D. Zhu, *Chem. Soc. Rev.*, 2010, **39**, 2411–2419.
19 E. Betzig, G. H. Patterson, R. Sougrat, O. W. Lindwasser, S. Olenych, J. S. Bonifacino, M. W. Davidson, J. Lippincott-Schwartz and H. F. Hess, *Science*, 2006, **313**, 1642–1645.
20 B. Dubertret, P. Skourides, D. J. Norris, V. Noireaux, A. H. Brivanlou and A. Libchaber, *Science*, 2002, **298**, 1759–1762.
21 B. N. G. Giepmans, S. R. Adams, M. H. Ellisman and R. Y. Tsien, *Science*, 2006, **312**, 217–224.
22 A. M. Smith, H. Duan, A. M. Mohs and S. Nie, *Adv. Drug Delivery Rev.*, 2008, **60**, 1226–1240.
23 A. Bhirde, J. Xie, M. Swierczewska and X. Chen, *Nanoscale*, 2011, **3**, 142–153.
24 Z. Chi, X. Zhang, B. Xu, X. Zhou, C. Ma, Y. Zhang, S. Liu and J. Xu, *Chem. Soc. Rev.*, 2012, **48**, 3878–3896.
25 X. Zhang, Z. Chi, B. Xu, C. Chen, X. Zhou, Y. Zhang, S. Liu and J. Xu, *J. Mater. Chem.*, 2012, **22**, 18505–18513.
26 C. Chen, J.-Y. Liao, Z. Chi, B. Xu, X. Zhang, D.-B. Kuang, Y. Zhang, S. Liu and J. Xu, *J. Mater. Chem.*, 2012, **22**, 8994–9005.
27 X. Zhou, H. Li, Z. Chi, X. Zhang, J. Zhang, B. Xu, Y. Zhang, S. Liu and J. Xu, *New J. Chem.*, 2012, **36**, 685–693.
28 R. Zhan, A. J. H. Tan and B. Liu, *Polym. Chem.*, 2011, **2**, 417–421.
29 K. Li, J. Pan, S. S. Feng, A. W. Wu, K. Y. Pu, Y. Liu and B. Liu, *Adv. Funct. Mater.*, 2009, **19**, 3535–3542.
30 J. Liu, D. Ding, J. Geng and B. Liu, *Polym. Chem.*, 2012, **3**, 1567–1575.
31 A. Qin, J. W. Lam and B. Z. Tang, *Prog. Polym. Sci.*, 2012, **37**, 182–209.

32 Z. Wang, B. Xu, L. Zhang, J. Zhang, T. Ma, J. Zhang, X. Fu and W. Tian, *Nanoscale*, 2013, **5**, 2065–2072.
33 H. Lu, B. Xu, Y. Dong, F. Chen, Y. Li, Z. Li, J. He, H. Li and W. Tian, *Langmuir*, 2010, **26**, 6838–6844.
34 Y. Hong, J. W. Lam and B. Z. Tang, *Chem. Commun.*, 2009, 4332–4353.
35 Y. Hong, J. W. Lam and B. Z. Tang, *Chem. Soc. Rev.*, 2011, **40**, 5361–5388.
36 D. Ding, K. Li, B. Liu and B. Z. Tang, *Acc. Chem. Res.*, 2013, DOI: 10.1021/ar3003464.
37 W. Qin, D. Ding, J. Liu, W. Z. Yuan, Y. Hu, B. Liu and B. Z. Tang, *Adv. Funct. Mater.*, 2012, **22**, 771–779.
38 X. Zhang, X. Zhang, S. Wang, M. Liu, L. Tao and Y. Wei, *Nanoscale*, 2013, **5**, 147–150.
39 X. Zhang, X. Zhang, B. Yang, S. Wang, M. Liu, Y. Zhang and L. Tao, *RSC Adv.*, 2013, **3**, 9633–9636.
40 D. Li, J. Yu and R. Xu, *Chem. Commun.*, 2011, **47**, 11077–11079.
41 X. Zhang, X. Zhang, S. Wang, M. Liu, Y. Zhang, L. Tao and Y. Wei, *ACS Appl. Mater. Interfaces*, 2013, **5**, 1943–1947.
42 X. Zhang, X. Zhang, B. Yang, M. Liu, W. Liu, Y. Chen and Y. Wei, *Polym. Chem.*, 2013, **4**, 4317–4321.
43 D. Li, Z. Liang, J. Chen, J. Yu and R. Xu, *Dalton Trans.*, 2013, **42**, 9877–9883.
44 A. M. Breul, M. D. Hager and U. S. Schubert, *Chem. Soc. Rev.*, 2013, **42**, 5366–5407.
45 X. Zhang, J. Hui, B. Yang, Y. Yang, D. Fan, M. Liu, L. Tao and Y. Wei, *Polym. Chem.*, 2013, **4**, 4120–4125.
46 X. Zhang, C. Fu, L. Feng, Y. Ji, L. Tao, Q. Huang, S. Li and Y. Wei, *Polymer*, 2012, **53**, 3178–3184.
47 Y. Zhu, W. Li, Q. Li, Y. Li, X. Zhang and Q. Huang, *Carbon*, 2009, **47**, 1351–1358.
48 X. Zhang, Y. Zhu, J. Li, Z. Zhu, W. Li and Q. Huang, *J. Nanopart. Res.*, 2011, **13**, 6941–6952.
49 X. Zhang, J. Yin, C. Peng, W. Hu, Z. Zhu, W. Li, C. Fan and Q. Huang, *Carbon*, 2011, **49**, 986–995.
50 X. Zhang, J. Yin, C. Kang, J. Li, Y. Zhu, W. Li, Q. Huang and Z. Zhu, *Toxicol. Lett.*, 2010, **198**, 237–243.
51 L. Zhan, G. Yanxia, Z. Xiaoyong, Q. Wei, F. Qiaohui, L. Yan, J. Zongxian, W. Jianjun, T. Yuqin, D. Xiaojiang and W. Wangsuo, *J. Nanopart. Res.*, 2011, **13**, 2939–2947.
52 J. Li, Y. Zhu, W. Li, X. Zhang, Y. Peng and Q. Huang, *Biomaterials*, 2010, **31**, 8410–8418.
53 L. Xu, X. Zhang, C. Zhu, Y. Zhang, C. Fu, B. Yang, L. Tao and Y. Wei, *J. Biomater. Sci., Polym. Ed.*, 2013, **24**, 1564–1574.
54 X. Zhang, H. Qi, S. Wang, L. Feng, Y. Ji, L. Tao, S. Li and Y. Wei, *Toxicol. Res.*, 2012, **1**, 201–205.
55 X. Zhang, W. Hu, J. Li, L. Tao and Y. Wei, *Toxicol. Res.*, 2012, **1**, 62–68.
56 Y. Zhu, X. Zhang, J. Zhu, Q. Zhao, Y. Li, W. Li, C. Fan and Q. Huang, *Int. J. Mol. Sci.*, 2012, **13**, 12336–12348.
57 Y. Zhang, B. Yang, X. Zhang, L. Xu, L. Tao, S. Li and Y. Wei, *Chem. Commun.*, 2012, **48**, 9305–9307.
58 B. Yang, Y. Zhang, X. Zhang, L. Tao, S. Li and Y. Wei, *Polym. Chem.*, 2012, **3**, 3235–3238.
59 X. Zhang, S. Wang, C. Zhu, M. Liu, Y. Ji, L. Feng, L. Tao and Y. Wei, *J. Colloid Interface Sci.*, 2013, **397**, 39–44.
60 X. Zhang, S. Wang, M. Liu, J. Hui, B. Yang, L. Tao and Y. Wei, *Toxicol. Res.*, 2013, **2**, 335–342.